Near infrared in vitro measurements of photosystem I cofactors and electron- transfer partners with a recently-developed spectrophotometer

Pierre Sétif, Alain Boussac, Anja Krieger-Liszkay

Near infrared *in vitro* measurements of photosystem I cofactors and electron-transfer partners with a recently-developed spectrophotometer

Pierre Sétif, Alain Boussac and Anja Krieger-Liszkay

Institute for Integrative Biology of the Cell (I2BC), CEA, CNRS, Université Paris-Sud, Université Paris-Saclay, 91198 Gif-sur-Yvette cedex, France

Corresponding author: pierre.setif@cea.fr

Tel.: + 33 169089867

ORCID numbers:

Pierre Sétif: 0000-0002-6101-4006

Alain Boussac **:** 0000-0002-3441-3861

Anja Krieger-Liszkay: 0000-0001-7141-4129

Acknowledgements

A. K.-L. and P.S. most gratefully thank Dr. C. Klughammer for his help in installing the Klas-NIR spectrophotometer and in using the associated software. They also thank the LabEx Saclay Plant Sciences-SPS (ANR-10-LABX-0040-SPS) for its financial support for the acquisition of the Klas-NIR spectrophotometer. This work was also partially supported by the French Infrastructure for Integrated Structural Biology (FRISBI, ANR-10-INBS-05a) and by a grant from the Agence Nationale de la Recherche (RECYFUEL project, ANR-16-CE05-0026).

Abstract

A kinetic-LED-array-spectrophotometer (Klas) was recently developed for measuring *in vivo* redox changes of P700, plastocyanin (PCy) and ferredoxin (Fd) in the near-infrared (NIR). This spectrophotomer is used in the present work for *in vitro* light-induced measurements with various combinations of photosystem I (PSI) from tobacco and 2 different cyanobacteria, spinach plastocyanin, cyanobacterial cytochrome c_6 (cyt. c_6) and Fd. It is shown that cyt. c_6 oxidation contributes to the NIR absorption changes. The reduction of (F_A F_B), the terminal electron acceptor of PSI, was also observed and the shape of the (F_A F_B) NIR difference spectrum is similar to that of Fd. The NIR difference spectra of the electron-transfer cofactors were compared between different organisms and to those previously measured *in vivo* whereas the relative absorption coefficients of all cofactors were determined by using single PSI turnover conditions. Thus, the (840 nm *minus* 965 nm) extinction coefficients of the light-induced species (oxidized *minus* reduced for PC and cyt. c_6, reduced *minus* oxidized for (F_A F_B) and Fd) were determined with values of 0.207±0.004, -0.033±0.006, -0.036±0.008 and -0.021±0.005 for PCy, cyt. c_6, (F_A F_B) (single reduction) and Fd, respectively, by taking a reference value of +1 for $P700^+$. The fact that the NIR P700 coefficient is larger than that of PCy and much larger than that of other contributing species, combined with the observed variability in the NIR P700 spectral shape, emphasizes that deconvolution of NIR signals into different components requires a very precise determination of the P700 spectrum.

Keywords: P700, plastocyanin, cyt. c_6, photosystem I terminal acceptor, ferredoxin, deconvolution.

Introduction

Photosystem I (PSI) is a light-induced plastocyanin (or cytochrome c_6)-ferredoxin (or flavodoxin) oxidoreductase (Amunts et al. 2007; Jordan et al. 2001; Qin et al. 2015). Upon light excitation, the PSI reaction centers perform a charge separation which, within less than 1 µs, leads to the formation of $P700^+$ and singly-reduced (F_A F_B) on either side of the photosynthetic membrane (Brettel and Leibl 2001). P700 is a dimer of chlorophyll a/a' molecules (Nakamura et al. 2003) which is located on the C_2 pseudo-symmetry axis of the membrane heterodimeric core of PSI. The terminal electron acceptors F_A and F_B are two [4Fe-4S] clusters bound to a small extrinsic subunit. Under single charge separation, singly reduced (F_A F_B) (later named $(F_A\ F_B)_{1red}$) undergoes fast (sub-µs) redox equilibration between the state (F_{Ared}, F_{Box}) and (F_{Aox}, F_{Bred}) (Brettel and Leibl 2001; Sétif 2001). Stabilization of the charge-separated pair involves many steps and cofactors, among which a third [4Fe-4S] cluster named F_X which is on the electron transfer pathway between the 2 phylloquinones present in PSI (Srinivasan and Golbeck 2009) and F_A.

$P700^+$ is reduced by a soluble partner on the lumenal side of the membrane. This partner is plastocyanin (Pcy), a copper-containing protein, in chloroplasts of plants (Molina-Heredia et al. 2003). Pcy can be replaced by a soluble cytochrome, cytochrome c_6 (cyt. c_6), in algae and some cyanobacteria under conditions of copper deficiency (Merchant and Bogorad 1987; Zhang et al. 1992). Moreover, some cyanobacteria such as *Thermosynechococcus elongatus* (*T. elong.*) have no Pcy gene and therefore use only cyt. c_6 as the lumenal donor to $P700^+$ (http://genome.microbedb.jp/cyanobase/). After its reduction, $(F_A\ F_B)_{red}$ reduces a soluble partner on the stromal/cytoplasmic side of the membrane. This partner is Fd, a [2Fe-2S]-cluster-containing protein, which can be replaced in most cyanobacteria and many algae by flavodoxin, a flavin-containing protein, mostly under conditions of iron deprivation (Karlusich et al. 2014). During CO_2 assimilation, both PSI soluble partners are involved in linear and cyclic electron flows. Whereas Pcy and/or cyt. c_6 connect PSI to the cytochrome b_6/f complex, Fd_{red} can reduce, besides its major partner ferredoxin-$NADP^+$-oxidoreductase for $NADP^+$ reduction, many different partners involved in anabolic processes such as nitrogen and sulfur assimilation (Fukuyama 2004).

Among the real-time non-destructive spectroscopic tools used for investigating photosynthesis *in vivo*, pulse-amplitude modulation (PAM) techniques measuring chlorophyll fluorescence and P700 redox state are widely used (Schreiber et al. 1986; Schreiber et al. 1988). A new PAM-based measuring system was recently developed which allows, besides chlorophyll fluorescence detection, the simultaneous *in vivo* measurement of P700, Pcy and Fd absorption changes by deconvoluting near infrared (NIR) signals recorded at 5 different wavelengths (Klughammer and Schreiber 2016; Schreiber and Klughammer 2016; Schreiber 2017). The availability of both Pcy and Fd measurements with this technique open new possibilities for studying photosynthesis. Having this goal in mind, we considered both important and useful to use this technique for investigating PSI reactions *in vitro*. Such an approach has three main goals which take advantage of the relative simplicity of *in vitro* PSI *vs* the more complex *in vivo* situation: i) to quantify the relative signal sizes of the different electron-transfer carriers by studying single PSI turnover; ii) to investigate the potential and yet uncharacterized contribution to NIR signals of cyt. c_6 and (F_A F_B) and iii) to contribute to the validation of the deconvolution approach.

Materials and methods

Biological materials

Tobacco PSI was prepared as previously described (Caffarri et al. 2001) using β-dodecyl-maltoside instead of α-dodecyl-maltoside. PSI trimers from *T. elong.* were prepared by using anion exchange separation as previously described (Moal and Lagoutte 2012). PSI monomers from *Synechocystis* sp. PCC 6803 (*Syn*. 6803) were prepared as previously described (Rögner et al. 1990). Cyt. c_6 and Fd were purified from *T. elong.* by using a combination of chromatographies as previously described (Kerfeld

et al. 2003). Pcy was purified from spinach leaves as previously described (Christensen et al. 1991). Cyt. c_6 concentration was calculated by using an extinction coefficient (reduced *minus* oxidized) of 19 $mM^{-1}cm^{-1}$ for the α-band peak absorption (553 nm) *minus* the absorption minimum near 537 nm (Cho et al. 1999). Horse heart cyt. *c* concentration was calculated by using an extinction coefficient (reduced *minus* oxidized) of 21 $mM^{-1}cm^{-1}$ at the α-band maximum (Massey 1959; Vangelder and Slater 1962). Pcy concentration was calculated using an absorption coefficient of 4.9 $mM^{-1}cm^{-1}$ at 597 nm for its oxidized form (Katoh et al. 1962). Fd concentration was calculated using an absorption coefficient of 9.7 $mM^{-1}cm^{-1}$ at 422 nm for its oxidized form (Tagawa and Arnon 1968). The concentration of *T. elong.* PSI was measured with laser flash-absorption spectroscopy using a $P700^+$ absorption coefficient of 7.7 $mM^{-1}cm^{-1}$ at 800 nm (Cassan et al. 2005). In the case of tobacco PSI, there is, to our knowledge, no precise determination of the $P700^+$ absorption coefficient in the NIR. The PSI concentration was then calculated by assuming that the $P700^+$ Klas-NIR absorption pseudo-coefficient at 902.5 nm (*i.e*. the difference between the coefficients at 840 nm and 965 nm) was identical to that of *T. elong.* $P700^+$, as supported by experiments in the present work (see Results). From laser flash-absorption measurements of tobacco $P700^+$ at 800 nm made in parallel with the Klas-NIR measurements, this assumption results in an absorption coefficient of 6.7 $mM^{-1}cm^{-1}$ for tobacco $P700^+$ at 800 nm (Table 1), in close agreement with a previous rough estimation (6.5 $mM^{-1}cm^{-1}$ at 820 nm, Mathis and Sétif 1981). All flash-absorption and Klas-NIR measurements were performed in Tricine 20 mM pH 8, in the presence of 0.03% β-dodecylmaltoside, 5 mM $MgCl_2$ and 30 mM NaCl.

Redox difference spectra using (UV)-visible spectroscopy

Redox difference spectra of cyt. c_6, horse heart cytochrome *c* (Sigma-Aldrich) and Fd were measured with a Uvikon XS spectrophotometer using Hellma microcuvettes (100 µl volume, 1-cm pathlength). Cytochromes at 600 µM concentrations were reduced and oxidized with 2 mM sodium ascorbate and 2 mM potassium ferricyanide, respectively. Cytochromes at 60 µM concentrations were reduced and oxidized with 200 µM sodium ascorbate and 200 µM potassium ferricyanide, respectively. In the case of Fd, a *c*. 450 µM Fd solution was buffered at pH 9 (50 mM AMPSO), deoxygenated by prolonged incubation in a glove box under a N_2 atmosphere (< 10 ppm O_2) and then reduced by 3 mM sodium dithionite.

Laser flash-absorption spectroscopy

Flash-absorption microscopy with microsecond time resolution was performed as previously described (Sétif et al. 2017). In brief, samples were contained in 1 × 1 cm cuvettes and electron transfer was triggered by PSI photoexcitation with a nanosecond laser flash. Continuous absorption detection was made at individual wavelengths which are selected by interference filters. When measuring in the visible region, the actinic effect of the measuring light was minimized by using a shutter placed in front of the cuvette and opened 1 ms before the laser flash.

Klas-NIR measurements

Measurements were made with a kinetic-LED-array-spectrophotometer (Klas) using NIR measuring lights with pulse-amplitude modulation (Klughammer and Schreiber 2016; Schreiber and Klughammer 2016; Schreiber 2017). Signal deconvolution between different spectral components is made from 4 light-induced differential signals which are obtained from the measurements at 5 different wavelengths by taking advantage of the fact that the components to be deconvoluted exhibit different NIR spectra. These 5 wavelengths are 780, 820, 840, 870 and 965 nm and the 4 difference signals are (780 nm - 820 nm, middle wavelength 800 nm), (820 nm - 870 nm, middle wavelength 845 nm), (840 nm - 965 nm, middle wavelength 902.5 nm) and (870 nm - 965 nm, middle wavelength 917.5 nm). After spectral deconvolution, the amplitudes of the different components (P700, PCy, cyt. c_6, Fd, (F_A F_B)) correspond to their respective contributions to the absorption changes

at 902.5 nm and are given in ($\Delta I/I \times 10^3$) (*i.e*. $\Delta A \times 2.3\ 10^3$). In the course of this study, we will measure the differential absorption coefficient of one species relative to another and more specifically of all species relative to $P700^+$, at the reference wavelength of 902.5 nm.

Measurements were made in the "Slow Kinetics" mode together with the "High Resolution Triggering Run" option with data acquisition every ms. So called single turnover (ST) pulses (at 624 nm) of 50 µs duration were used in most cases for PSI excitation. These 50 µs flashes were checked to be saturating PSI photochemistry by verifying that the photoproduced $P700^+$ amplitude after 25 µs flashes was the same. The 50 µs flashes were generally inducing single PSI turnover, because electron donation to $P700^+$ was in most cases more than one order of magnitude slower than 50 µs. There was an exception to this when studying tobacco PSI with spinach plastocyanin as faster $P700^+$ reduction by Pcy was occurring. In this case, a laser flash (6 ns duration, 700 nm, energy > 15 mJ) was used, which was both saturating and single turnover. The laser flash was synchronized with Klas-NIR data acquisition using the external trigger output of the spectrophotometer.

Comparison of $P700^+$ signal amplitudes measured by laser-flash absorption spectroscopy and with the Klas-NIR spectrophotometer

The $P700^+$ signal was first measured at 800 nm by flash-absorption spectroscopy in the presence of ascorbate/DCPIP and MV (under these conditions, $P700^+$ is the only species present after a few ms) with purified PSI from *Syn*. 6803, *T. elong.* and tobacco. For both cyanobacterial PSIs, an absorption coefficient of 7.7 $mM^{-1}cm^{-1}$ was measured (Cassan et al. 2005). The same samples were then studied with the Klas-NIR spectrophotometer using a saturating single-turnover flash. From the absorption changes measured at 845 nm (820 nm – 870 nm) and 902.5 nm (840 nm – 965 nm), the Klas-NIR pseudo-coefficients were obtained (Table 1). As discussed above, it was assumed that the pseudo-coefficient of tobacco $P700^+$ is identical to that of *T. elong.* at 902.5 nm. The other coefficients of tobacco $P700^+$ were calculated using this assumption.

Results

Pseudospectra of PSI components and electron-transfer partners.

By studying with the Klas-NIR spectrophotometer *in vitro* mixtures of PSI and its redox partners Pcy, cyt. c_6 and Fd, we measured light-induced redox-difference spectra of these partners and of the P700 and (F_A F_B) cofactors (Fig. 1). These pseudospectra, called differential model plots in (Klughammer and Schreiber 2016; Schreiber and Klughammer 2016; Schreiber 2017) and reference spectra in the following, were measured under conditions where a single component can be observed without any other contribution, as explained in the case of *in vivo* measurements for P700, Pcy and Fd (Klughammer and Schreiber 2016). As compared to *in vivo* determinations, such conditions are relatively easy to get *in vitro*, which facilitates these determinations. Such conditions will be given in the paragraphs below during the description of individual experiments. Moreover, *in vitro* experiments allowed us to measure signals under single PSI turnover conditions, from which the relative signal amplitudes of the different species can be determined. One can also note that Klas-NIR spectra of cyt. c_6 and (F_A F_B) were newly determined in the present study, which can be of interest for future *in vivo* studies.

$P700^+$ reference spectra shown in Fig. 1A were measured with PSI from two cyanobacteria, *Syn*. 6803 (spectrum 1) and *T. elong*. (spectrum 2) and from tobacco (spectrum 3). Whereas these 3 spectra are different one from the other two, the tobacco spectrum is very similar to that determined *in vivo* in *Helianthus annuus* (spectrum 4, provided with the Klas-NIR software). Reference spectra of all species from *T. elong*. plus Pcy from spinach are shown in Fig. 1B, after normalisation of their amplitudes at 902.5 nm, which allows shape comparison. The same spectra are shown with their signed relative amplitudes in Fig. 1C, by assuming a reference value of 1 for $P700^+$ at 902.5 nm (not shown in Fig. 1C). The Fig. 1C spectra correspond to the light-induced differences, *i.e*. oxidized minus

reduced for PCy and cyt. c_6 (spectra d and e, respectively) and reduced minus oxidized for Fd and (F_A F_B) (spectra b and c, respectively). The spectra of Fig. 1C are also shown individually in Fig. SI1 together with their *Helianthus annuus* counterparts (for Pcy and Fd) that are provided with the Klas-NIR software. From these spectra, it appears that the *in vitro* spinach Pcy reference spectrum is very similar to that measured in *Helianthus annuus* leaves whereas the *in vitro T. elong.* Fd reference spectrum is somewhat different from that measured in these leaves.

Several features emerge from spectral comparisons of the different electron-transfer components. Firstly, $P700^+$ exhibits by far the largest amplitudes at all wavelengths except 800 nm. Then Pcy is second in size, except at 800 nm, with its oxidation signal at 902.5 nm being *c*. 5-fold smaller than that of P700. As compared to Pcy, cyt. c_6 oxidation gives a signal of opposite sign at 902.5 nm, with the absolute amplitude at this wavelength being *c*. 30-fold smaller than that of P700. Fd and (F_A F_B) reductions (single reduction is considered here in the case of the 2-electrons carrier (F_A F_B)) give signals of similar shapes but with a larger negative amplitude at 902.5 nm for (F_A F_B). Absolute amplitudes of Fd and (F_A F_B) at this wavelength are *c*. 50-fold and 30-fold smaller than that of $P700^+$, respectively.

It should be noted that the Pcy signal amplitude could only be determined by reference to tobacco $P700^+$, due a poor reactivity of spinach Pcy with cyanobacterial PSI, which impedes a precise quantitative signal comparison with cyanobacterial $P700^+$. However, all other species were determined with PSI of both tobacco and *T. elong*. From the results, listed in Table 2, it appears that the amplitude factors at 902.5 nm are quite similar for cyt. c_6, (F_A F_B) and Fd when measured by reference to *T. elong*. $P700^+$ or tobacco $P700^+$. In turn, this indicates that the 902.5 nm absorption pseudo-coefficient of $P700^+$ is quite similar for the 2 species, so that the Pcy amplitude factor measured by reference to tobacco $P700^+$ can be extrapolated to *T. elong.* $P700^+$.

Relative amplitudes of P700 from tobacco and plastocyanin from spinach.

In isolated PSI in the presence of MV, light-induced charge separation is followed by fast oxidation of $(F_A, F_B)_{1red}$ by MV so that $P700^+$ is rapidly the only remaining light-induced species. Klas-NIR absorption changes were recorded under such conditions with tobacco PSI using nanosecond laser excitation. In the presence of 1 mM MV, $(F_A, F_B)_{red}$ is oxidized in the subms time-range (Ke 1973; Sétif 2015). Thus, the absorption changes at the 4 middle wavelengths are homothetic (data not shown), in accordance with the fact that only $P700^+$ is present. The decaying signals correspond to slow reduction of $P700^+$ by ascorbate-reduced DCPIP (trace a of Fig. 2A) and were therefore used to get the reference spectrum of ($P700^+$ - P700) (*i.e.* of $P700^+$, as P700 does not contribute to NIR absorption changes).

Addition of *c*. 8 µM Pcy to the above sample leads to fast $P700^+$ decay and formation of oxidized Pcy (Pcy^+) (traces b and c of Fig. 2A). For this 2-species deconvolution (P700 and Pcy) of the Klas-NIR signals, we used the above $P700^+$ reference spectrum and a (Pcy^+ - Pcy) reference spectrum that was measured with the same sample and a multiple turnover flash of 5 ms duration (data not shown). With such an illumination, the extent of Pcy^+ oxidation is increased and the relative contribution of the non Pcy-reducible part of $P700^+$ (see below) is minimized. With the nanosecond laser flash excitation that is used in Fig. 2A, single PSI turnover is expected as reduction of $P700^+$ by Pcy occurs in the microsecond/millisecond timescale with the fastest phase, due to PSI:Pcy intracomplex electron transfer, exhibiting a halftime of a few µs (Drepper et al. 1996). Whereas most of $P700^+$ has fully decayed within 6 ms (with part of the decay being not time-resolved and most probably occurring in the µs time range), a small residual signal (5.5% of the initial $P700^+$ signal) decays very slowly (trace c). The reference spectrum of this slowly-decaying species was measured at 2 s, a time at which Pcy^+ has fully decayed, and its spectrum is very similar although not identical to that of the major part of $P700^+$ (data not shown). These data suggest that *c*. 5% of $P700^+$ is not reducible by Pcy in our PSI preparation. Whereas Pcy oxidation is completed within a few ms, Pcy^+ decays slowly in hundreds of ms (trace b). This decay is attributed to reduction of Pcy^+ by ascorbate and/or reduced

DCPIP. Both $P700^+$ (trace a, in the absence of Pcy) and Pcy^+ (trace b) decays were fitted with monoexponential functions (black curves). By using the initial amplitudes of these exponential decays (2.57 and 0.51 for $P700^+$ and Pcy^+, respectively) and by taking into account the fact that 95% of $P700^+$ is reduced by Pcy, a value of 0.21 (= 0.51/(2.57*0.95)) was estimated for the Pcy to P700 signals ratio at 902.5 nm.

In another experiment (Fig. 2B) using also single laser flash excitation, a smaller Pcy concentration (*c*. 0.8 µM) was added to PSI (in the presence of 1 mM MV). Under these conditions, $P700^+$ reduction by Pcy is essentially second-order and most of it is slow enough to be time-resolved. The detectable part of the $P700^+$ decay (trace d) is biexponential with a major fast component attributed to reduction by Pcy and a minor component due to the Pcy-non reducible part of $P700^+$. Pcy^+ signal rise has two components, a small unresolved one attributed to ET occurring in a small proportion of PSI with bound Pcy and a major one with rising kinetics similar to the $P700^+$ major decay kinetics. From a global fit of these data (black curves), a rate of 73.5 s^{-1} was obtained for the component common to $P700^+$ decay and Pcy^+ rise. By assuming first-order approximation ([Pcy] >> [PSI]), a second-order rate constant of 9.2×10^7 $M^{-1}s^{-1}$ (= 73.5 s^{-1}/0.8 µM) can be calculated for $P700^+$ reduction by Pcy, in relative agreement with those measured with spinach PSI ($1.1\text{-}3.5 \times 10^8$ $M^{-1}s^{-1}$; Drepper et al. 1996). By comparing the preexponential factors of the 73.5 s^{-1} component in the $P700^+$ and Pcy^+ kinetics, a value of 0.204 was estimated for the Pcy to P700 amplitudes ratio, which is quite similar to the one obtained from the data of Fig. 2A. Another way of illustrating the relative sizes of the Pcy^+ and $P700^+$ signals of Fig. 2B is to plot Pcy^+ as a function of $P700^+$. This was made from the signals recorded between 0 and 100 ms after the flash in Fig. 2C, where the straight line corresponds to a signal ratio ($Pcy^+/P700^+$) of 0.204.

Cytochrome c_6 oxidation gives absorption changes in the NIR region.

In this part, we used PSI and cyt. c_6 purified from *T. elong*. As in the preceding paragraph, PSI alone with the addition of MV was used to get the $P700^+$ reference spectrum. The $P700^+$ decay kinetics is shown in trace a of Fig. 3A, after excitation with a 50 µs single turmover pulse. After addition of cyt. c_6 at a concentration of 8.3 µM, $P700^+$ was found to decay with a halftime of about 15 ms with no faster phase which would correspond to the presence of some PSI:cyt. c_6 complex (trace b). The absence of such a complex was checked with a cyt. c_6 concentration up to 25 µM by flash-absorption spectroscopy by probing $P700^+$ decay with a µs time resolution. No microsecond phase indicative of fast intracomplex ET was observed in these control measurements (data not shown), indicating that, under the present conditions, a 50 µs pulse elicits single PSI turnover.

However, it was also observed that the absorption changes could not be satisfactory fitted assuming that only $P700^+$ is contributing because of the presence of small slowly-decaying signals which are present after the expected completion of $P700^+$ decay and which are negative at all wavelengths differences except at (780 nm – 820 nm). These slow signals were presumably due to cyt. c_6 oxidation. This result was unexpected as, to our knowledge, redox absorption changes in the near-infrared have not been reported for c-type cytochromes yet. The cyt. c_6 reference spectrum (cyt. c_6^+ - cyt. c_6) was obtained from the time domain where $P700^+$ has fully decayed via its reduction by cyt. c_6 (traces c and d), especially with the largest signal obtained after a series of 4 consecutive 50 µs flashes (separated by 100 ms time intervals, trace d). Some short-lasting spikes of unknown origin ending at *c*. 60 ms are also present just after light excitation in the cyt. c_6 deconvoluted signals. Cyt. c_6 kinetics were fitted with a single exponential decay using data only after 60 ms after the last flash (black curves). From the single flash fit extrapolated to time 0, a value of -0.039 was obtained for the cyt. c_6 to P700 ratio (*i.e*. the ratio of the differential absorption pseudo-coefficients at 902.5 nm).

It was also found that the further addition of DCPIP (which is reduced by ascorbate) leads to the rapid decay of cyt. c_6^+ (trace c' of Fig. 3B = cyt. c_6 signal after 2-species deconvolution). Under such conditions (MV, cyt. c_6, DCPIP), all NIR signals thus vanish rapidly within 20-30 ms after the flash. Reduction of cyt. c_6^+ by reduced DCPIP was checked in the visible region by flash-absorption

spectroscopy with microsecond time resolution (see Fig. SI2). These experiments were showing that under the conditions of Fig. 3B, cyt. c_6^+ should not accumulate, in accordance with the Klas-NIR data.

Absorption of cyt. c_6 in the NIR region was checked by measuring its redox difference spectrum with a UV-visible spectrophotometer (Fig. 4, reduced *minus* oxidized spectra). This is shown not only for cyt. c_6 (A and B) but also for horse heart cyt. *c* (C and D) with similar Fe axial ligands (His and Met). Whereas the α and β bands are shown in parts A and C, a wide band of weak intensity ($\Delta\varepsilon \geq 200$ $M^{-1}cm^{-1}$) is visible around 800 nm for both cytochromes (parts B and D). From these spectra, cyt. c_6 oxidation is expected to lead to a small absorption bleaching upon oxidation at 902.5 nm (840 minus 965 nm), in accordance with the Klas-NIR observations.

The (F_A, F_B) redox difference spectrum is similar to that of Fd in NIR.

It has been previously shown that [4Fe-4S] clusters exhibit redox-dependent absorption changes in the NIR region (Stephens et al. 1978), as is the case for [2Fe-2S] clusters (Eaton et al. 1971; Rawlings et al. 1974). Therefore, we checked the contribution of (F_A, F_B) to infrared absorption changes by measuring the reoxidation of flash-induced singly reduced $(F_A, F_B)_{1red}$ by 400 µM MV from 730 to 1020 nm (Fig. SI3). For each of the two PSI samples that were studied, the kinetics were analyzed by a global fitting procedure which resulted in the data of Fig. 5 (black symbols). In the presence of an excess of Fd, Fd is reduced from $(F_A, F_B)_{1red}$ without significant competition of MV reduction when 200 µM MV is used (Fig. SI3). Fd_{red} is then rapidly oxidized by MV (Sétif 2015). In this case as well, a global fitting procedure was used with each of the two samples (Fig. 5, red symbols). These experiments with Fd allowed us to compare the signal amplitudes of the flash-absorption data to the redox difference spectrum obtained by chemical reduction with sodium dithionite (Fig. 5, orange continuous line). Whereas both measurements give, as expected, similar signals for Fd, the flash measurements show that (F_A, F_B) reduction also gives contributions to NIR absorption. (F_A, F_B) and Fd spectral shapes are similar with a larger amplitude for (F_A, F_B) at most wavelengths, in accordance with the larger size of the (F_A F_B) reference spectrum (Fig. 1C).

Comparison of (F_A, F_B) and Fd signals in Klas-NIR flash measurements.

Reference spectra of (F_A F_B) and Fd can be obtained under conditions where the PSI donor side gives no contribution. Such a situation is occurring in the presence of both cyt. c_6, which rapidly reduces $P700^+$ and ascorbate-reduced DCPIP, which rapidly reduces cyt. c_6^+. Fig. 6 presents data resulting from such experiments after 3-species deconvolution either in the absence of Fd (part A) or in its presence (part B). Signals from single or multiple 50 µs flashes were compared with signal amplitudes increasing with the number of flashes. A time separation between consecutive flashes of 20 ms ensures that most of $P700^+$ is reduced before the next flash (see inset in part A). In the absence of Fd, 3-species deconvolution involves $P700^+$, cyt. c_6 and (F_A F_B) whereas it involves P700, cyt. c_6 and Fd in its presence as Fd is reduced by $(F_A\ F_B)_{1red}$ in the submillisecond time range with 10 µM Fd (Sétif et al. 2017). Reference spectra of either (F_A F_B) (in the absence of Fd) or Fd (in its presence) were determined using signals measured more than 80 ms after the last flash, in order to avoid any error due to initial signal distortions of unknown origin which are present up to 50 ms after the flash(es) (Fig. 6A/B). These signal distortions indicate that deconvolution is not satisfactory shortly after the flash. This may be due *e.g.* to contributions of ascorbate and/or DCPIP radical species at short times.

The $(F_A\ F_B)_{red}$ signal size increases with the number of flashes (1, 2, 3 and 5 in Fig. 6A) up to the 3rd flash and then remains almost the same for 5 flashes, as seen by the signals at t > 50 ms. These signals were fitted with monoexponential fits, giving as well a flash-number saturating-like behavior (Fig. 6D) with an almost constant decay rate (Fig. 6C). As $P700^+$ and cyt. c_6^+ rapidly disappear and are thus not available for recombination reactions (see however below the case of multiple flash measurements), the $(F_A\ F_B)_{red}$ decay is attributed to its oxidation by oxygen (Mignée et al. 2017). The flash-number dependence of the amplitude is consistent with the presence of two [4Fe-4S], F_A and F_B, which can be relatively easily reduced. However, the saturated signal amplitude is less than twice

that of the single flash (0.12 *vs* 0.07), which is not consistent with the full accumulation of the doubly-reduced state (F_{Ared}, F_{Bred}). This discrepancy may have two origins. Firstly, the accumulation of (F_{Ared}, F_{Bred}) is not complete due to recombination with $P700^+$ ($t_{1/2} \approx 10$ ms, Jordan et al. 1998). Under these conditions, cyt. c_6 donation to $P700^+$ is not fast enough to lead to full reduction of both F_A and F_B. Secondly, the $(F_A\ F_B)_{red}$ oxidation by oxygen may be biphasic with the doubly-reduced state decaying initially faster than the singly-reduced one. Whereas such a biphasic behavior is expected since only the most solvent-exposed F_B cluster is oxidized by oxygen (Diaz-Quintana et al. 1998), it cannot be probed in the present experiments because of the 50 ms dead time.

In contrast, the Fd signal amplitude exhibits no saturation-like behavior (Fig. 6B/D), as expected from the fact that Fd_{red} can be photoaccumulated under the present conditions where Fd is in large excess over PSI. The Fd_{red} decay rate is flash-number independent and much slower than that of $(F_A\ F_B)_{red}$ (Fig. 6C), as expected from the poor reactivity of Fd_{red} with oxygen (Hosein and Palmer 1983).

The ($F_A\ F_B$) (single reduction) and Fd signal amplitudes were obtained by fitting the single flash-kinetics by a single exponential decay and extrapolating the decay fits to time 0 (Fig. 6A/B). The ($F_A\ F_B$)/P700 and Fd/P700 ratios of pseudo-coefficients at 902.5 nm were calculated (Table 2) from these amplitudes and the $P700^+$ signal (= 1.91, inset of Fig. 6A). The measurements described in Figures 3 and 6 were repeated with tobacco PSI since cyt. c_6 also rapidly reduces $P700^+$ in this case ($t_{1/2} \approx 4$ ms for a cyt. c_6 concentration of 6 µM) (data not shown). This allowed us to estimate the cyt. c_6, ($F_A\ F_B$) and Fd coefficients relatively to that of tobacco $P700^+$ (Table 2).

Other examples of NIR signals deconvolution of single flash experiments.

Fig. 7A shows the result of 2-species deconvolution (P700 and ($F_A\ F_B$)) with PSI from *T. elong.* which was excited by a single turnover flash in the presence of ascorbate and DCPIP. Under these conditions, $P700^+$ decays slowly with 2 exponential phases (inset). The rate of the fastest phase is ($k_r + k_e$) (= 17.6 s^{-1}), with k_r corresponding to the recombination reaction between $P700^+$ and $(F_A\ F_B)_{1red}$ and k_e being the electron escape rate, *i.e*. oxidation of $(F_A\ F_B)_{1red}$ by oxygen (Diaz-Quintana et al. 1998; Mignée et al. 2017). The slowest phase is attributed to $P700^+$ reduction by reduced DCPIP in the part of PSI where electron escape has occurred. In this reaction scheme, it is expected that $(F_A\ F_B)_{1red}$ is fully reoxidized with a single exponential component of rate ($k_r + k_e$), in accordance with the good fit of its decay obtained with a single exponential of fixed rate equal to 17.6 s^{-1} (blue line). Fd at high concentration (15 µM) was then added to the cuvette, resulting in the kinetics of Fig. 7B from 2-species deconvolution with P700 and Fd ($P700^+$ in the inset and red trace a for Fd_{red}). Whereas $P700^+$ slowly decays *via* reduction by reduced DCPIP, Fd_{red} signal decays *via* oxidation with oxygen. This last decay was fitted with a single exponential (blue line). When divided by the $P700^+$ signal, the extrapolated initial amplitudes of $(F_A\ F_B)_{1red}$ (Fig. 7A) and Fd_{red} are -0.039 and -0.024, respectively, showing that the ($F_A\ F_B$) single reduction signal is larger than that of Fd by about 70 %, as we generally observed (Table 2). A small amount of MV (0.5 µM) was then added to the cuvette, leading to a strong acceleration of the Fd_{red} decay (green trace b in Fig. 7B), with a fitted rate of 9.9 s^{-1}. From this rate, a second-order rate constant of 2×10^7 $M^{-1}s^{-1}$ is obtained which is in the same range as the value of 1.2×10^7 $M^{-1}s^{-1}$ that was previously measured by flash-absorption spectroscopy with Fd from *Syn*. 6803 (Sétif 2015).

In Fig. 8, we performed a 3-species deconvolution (P700, cyt. c_6, ($F_A\ F_B$)) with PSI from *T. elong.* in the presence of cyt. c_6 but in the absence of DCPIP. After single flash excitation, $P700^+$ decays fast due to its reduction by cyt. c_6 (green trace a), whereas $(F_A\ F_B)_{1red}$ and cyt. c_6^+ decays are slower and easily observable (black trace b and magenta trace c, respectively). Fits of both traces with a single exponential lead to initial amplitudes of similar sizes, in accordance with our other observations (Table 2).

Discussion

In the present study, we determined *in vitro* the NIR spectral contributions of PSI and PSI partners by using the Klas-NIR spectrophotometer. Beside the already characterized light-induced spectra of P700, Pcy and Fd (Klughammer and Schreiber 2016; Schreiber and Klughammer 2016; Schreiber 2017), the cyt. c_6 and (F_A F_B) light-induced spectra were also observed and characterized. The unexpected existence of a cyt. c_6 signal was confirmed by the measurement of a small redox difference by classical UV-visible-NIR spectrophotometry. This contribution will therefore have to be taken into account in future *in vivo* studies of algae and cyanobacteria expressing mostly or only cyt. c_6 instead of Pcy. Moreover, cyt. *f* of the cytochrome b_6f complex may give a small contribution to *in vivo* Klas-NIR measurements, assuming it has spectral properties similar to those of cyt. c_6. When PCy is the lumenal electron donor, cyt. *f* contribution may be hardly observable at its NIR absorption is about 6-times smaller than that of Pcy (Table 2) whereas it may observed together with cyt. c_6 when this one is the lumenal soluble donor.

The evidence that (F_A F_B) single reduction gives a NIR contribution similar in shape and larger by *c*. 70% as compared to Fd reduction should also be considered in future *in vivo* studies in cases where light leads to a strongly reduced state of stromal acceptors.

By using single turnover conditions, we measured the absorption pseudo-coefficients of all species relative to that of $P700^+$ at 902.5 nm. It was thus found that Pcy, cyt. c_6 , (F_A F_B) and Fd difference spectra give signals which are *c*. 5, 30, 30 and 50-times smaller than the $P700^+$ signal, respectively. On the other hand, we obtained evidence that the spectral shape of $P700^+$ is variable, as also observed for the red bleaching due to P700 oxidation (Witt et al. 2003), and is significantly different in cyanobacteria (*Syn*. 6803 and *T. elong.*) and vascular plants (tobacco and previously measured in *Helianthus annuus*). It is also different in the 2 cyanobacterial PSIs that we studied. When considered together, the large size of the $P700^+$ signal and its variability indicate that it is needed to measure its spectrum with a high precision for a reliable signal deconvolution involving other cofactors. When Pcy is present, its precise spectral determination is also probably required for a reliable determination of signals of smaller intensities (Fd and (F_A F_B)).

Our data also show that under *in vivo* conditions where Fd_{red} accumulates, (F_A F_B) reduction will give a signal which may add to the Fd reduction signal. Both species exhibit similar, albeit not identical, spectra and the question can be asked whether both species can be observed together, *i.e*. additively, with 3-species deconvolution (P700, Pcy or cyt. c_6, Fd and/or (F_A F_B)). We tentatively checked this point by swapping the Fd and (F_A F_B) reference spectra in cases where either Fd or (F_A F_B) should contribute to the Klas-NIR signals (*i.e*. using the (F_A F_B) spectrum instead of Fd when only the Fd signal is involved and the other way around). This procedure showed that, whereas the P700 and Pcy (when present) signals are almost not changed, some small changes (at most 20% and in many cases less than 10% signal intensity at any time) were observed in the deconvoluted cyt. c_6 and Fd/(F_A F_B) signal amplitudes (Fig. SI4). We also changed the Fd and (F_A F_B) reference spectra measured here for the *Helianthus annuus* Fd spectrum which differs significantly from both spectra (Fig. SI1) and obtained similar small changes in cyt. c_6 and Fd/(F_A F_B) signal amplitudes. Therefore it appears that, for *in vivo* measurements, the precise determination of the Fd reference spectrum may be not critical for signal deconvolution (in contrast to that of P700) whereas (F_A F_B) may be observable together with Fd in an additive manner.

Another issue is whether the spectral shapes of the different species and the relative 902.5 nm pseudo coefficients that we determined can be used for *in vivo* investigations. Regarding the spectral shapes of $P700^+$ in vascular plants, the similarity in $P700^+$ signals between *in vitro* tobacco PSI and *Helianthus annuus* is encouraging but in view of the large size of the P700 signal, it is certainly worth to redetermine it in every type of leaf and *a fortiori* every type of cyanobacterium. The high similarity of the PCy spectral shapes *in vitro* (spinach Pcy) and *in vivo* (*Helianthus annuus*) suggests that the Pcy spectrum may be extrapolated from one case to another. Regarding the relative absorption coefficients of the different electron-transfer species, the possibility of extrapolation from *in vitro* to *in vivo* will depend on the optical pathlengths of the different compartments (membrane, lumen,

stroma/cytoplasm) which may be different (or not) due to light scattering and light refraction/reflexion at the interfaces between membranes and soluble compartments. Some of these issues are addressed in the accompanying paper (Shimakawa et al., 2019).

PSI purified from	ε at 800 nm	ε at 845 nm (820 nm - 870 nm)	ε at 902.5 nm (840 nm - 965 nm)
T. elong.	7.7[(a)]	4.50[(b)]	4.75[(b)]
Syn. 6803	7.7[(a)]	4.25[(b)]	3.9[(b)]
tobacco	6.7[(d)]	3.75	4.75[(c)]

Table 1. Absorption and pseudo-absorption coefficients of $P700^+$ measured in 3 different PSI preparations.

All coefficients are given in $mM^{-1}cm^{-1}$.
[(a)]Previously measured by flash-absorption spectroscopy (Cassan et al. 2005).
[(b)]Measured with Klas-NIR, by comparing on the same sample the Klas-NIR signal to that measured at 800 nm by flash-absorption spectroscopy.
[(c)]Assumed to be identical to that of *T. elong.*
[(d)]Measured with flash-absorption spectroscopy, by comparing on the same sample this signal to that measured at 902.5 nm with Klas-NIR.

	Absorption pseudo-coefficients at 902.5 nm by reference to *T. elong*. $P700^+$	Absorption pseudo-coefficients at 902.5 nm by reference to tobacco $P700^+$
$P700^+$	1	1
Pcy_{ox} - Pcy_{red}	n.d.[(a)]	0.207 ± 0.004
cyt. c_{6ox} – cyt. c_{6red}	-0.033 ± 0.006	-0.034 ± 0.004
$(F_A\ F_B)_{1red}$ - $(F_A\ F_B)_{ox}$	-0.036 ± 0.008	-0.0335 ± 0.004
Fd_{red} - Fd_{ox}	-0.021 ± 0.005	-0.020[(b)]

Table 2. Relative differential absorption coefficients at 902.5 nm (840 nm *minus* 965 nm).

Standard deviations correspond to averages of 2 to 4 measurements.
[(a)]Not determined as the oxidation of spinach Pcy by $P700^+$ from *T. elong.* is slow and largely mixed with reduction of Pcy^+ by ascorbate.
[(b)]Single measurement.

REFERENCES

Amunts, A, Drory, O, Nelson, N (2007) The structure of a plant photosystem I supercomplex at 3.4 angstrom resolution. Nature 447:58-63

Brettel, K and Leibl, W (2001) Electron transfer in photosystem I. Biochim Biophys Acta 1507:100-114

Caffarri, S, Croce, R, Breton, J, Bassi, R (2001) The major antenna complex of photosystem II has a xanthophyll binding site not involved in light harvesting. J Biol Chem 276:35924-35933

Cassan, N, Lagoutte, B, Sétif, P (2005) Ferredoxin-$NADP^+$ reductase: Kinetics of electron transfer, transient intermediates, and catalytic activities studied by flash-absorption spectroscopy with isolated photosystem I and ferredoxin. J Biol Chem 280:25960-25972

Cho, YS, Wang, QJ, Krogmann, D, Whitmarsh, J (1999) Extinction coefficients and midpoint potentials of cytochrome c(6) from the cyanobacteria Arthrospira maxima, Microcystis aeruginosa, and Synechocystis 6803. Biochim Biophys Acta 1413:92-97

Christensen, HEM, Conrad, LS, Ulstrup, J (1991) Isolation and Purification of Plastocyanin from Spinach Stored Frozen Using Hydrophobic Interaction and Ion-Exchange Chromatography. Photosynth Res 28:89-93

Diaz-Quintana, A, Leibl, W, Bottin, H, Sétif, P (1998) Electron transfer in photosystem I reaction centers follows a linear pathway in which iron-sulfur cluster F_B is the immediate electron donor to soluble ferredoxin. Biochemistry 37:3429-3439

Drepper, F, Hippler, M, Nitschke, W, Haehnel, W (1996) Binding Dynamics and Electron Transfer between Plastocyanin and Photosystem I. Biochemistry 35:1282-1295

Eaton, WA, Palmer, G, Fee, JA, Kimura, T, Lovenberg, W (1971) Tetrahedral iron in the active center of plant ferredoxins and beef adrenodoxin. Proc Natl Acad Sci U S A 68:3015-3020

Fukuyama, K (2004) Structure and function of plant-type ferredoxins. Photosynth Res 81:289-301

Hosein, B and Palmer, G (1983) The kinetics and mechanism of oxidation of reduced spinach ferredoxin by molecular oxygen and its reduced products. Biochim Biophys Acta 723:383-390

Jordan, P, Fromme, P, Witt, HT, Klukas, O, Saenger, W, Krauss, N (2001) Three-dimensional structure of cyanobacterial photosystem I at 2.5 Å resolution. Nature 411:909-917

Jordan,R., Nessau,U., and Schlodder,E. (1998) Charge recombination between the reduced iron-sulphur clusters and $P700^+$. In Photosynthesis: Mechanisms and Effects, G.Garab, ed (Dordrecht: Kluwer Acad.. Publ.), pp. 663-666.

Karlusich, JJP, Lodeyro, AF, Carrillo, N (2014) The long goodbye: the rise and fall of flavodoxin during plant evolution. Journal of Experimental Botany 65:5161-5178

Katoh, S, Shiratori, I, Takamiya, A (1962) Purification and Some Properties of Spinach Plastocyanin. Journal of Biochemistry 51:32-&

Ke, B (1973) The primary electron acceptor of photosystem I. Biochim Biophys Acta 301:1-33

Kerfeld, CA, Sawaya, MR, Bottin, H, Tran, KT, Sugiura, M, Cascio, D, Desbois, A, Yeates, TO, Kirilovsky, D, Boussac, A (2003) Structural and EPR characterization of the soluble form of cytochrome c-550 and of the psbV2 gene product from the cyanobacterium Thermosynechococcus elongatus. Plant Cell Physiol 44:697-706

Klughammer, C and Schreiber, U (2016) Deconvolution of ferredoxin, plastocyanin, and P700 transmittance changes in intact leaves with a new type of kinetic LED array spectrophotometer. Photosynth Res 128:195-214

Massey, V (1959) The Microestimation of Succinate and the Extinction Coefficient of Cytochrome-C. Biochimica et biophysica acta 34:255-256

Mathis, P and Sétif, P (1981) Near infra-red absorption spectra of the chlorophyll *a* cations and triplet state in vitro and in vivo. Isr J Chem 21:316-320

Merchant, S and Bogorad, L (1987) Metal ion regulated gene expression: use of a plastocyanin-less mutant of *Chlamydomonas reinhardtii* to study the Cu(II)-dependent expression of cytochrome *c*-552. EMBO J 6:2531-2535

Mignée, C, Mutoh, R, Krieger-Liszkay, A, Kurisu, G, Sétif, P (2017) Gallium ferredoxin as a tool to study the effects of ferredoxin binding to photosystem I without ferredoxin reduction. Photosynth Res 134:251-263

Moal, G and Lagoutte, B (2012) Photo-induced electron transfer from photosystem I to $NADP^+$: Characterization and tentative simulation of the *in vivo* environment. Biochim Biophys Acta 1817:1635-1645

Molina-Heredia, FP, Wastl, J, Navarro, JA, Bendall, DS, Hervas, M, Howe, CJ, De la Rosa, MA (2003) A new function for an old cytochrome? Nature 424:33-34

Nakamura, A, Akai, M, Yoshida, E, Taki, T, Watanabe, T (2003) Reversed-phase HPLC determination of chlorophyll a' and phylloquinone in photosystem I of oxygenic photosynthetic organisms - Universal existence of one chlorophyll a' molecule in photosystem I. Eur J Biochem 270:2446-2458

Qin, X, Suga, M, Kuang, T, Shen, JR (2015) Photosynthesis. Structural basis for energy transfer pathways in the plant PSI-LHCI supercomplex. Science 348:989-995

Rawlings, J, Siiman, O, Gray, HB (1974) Low temperature electronic absorption spectra of oxidized and reduced spinach ferredoxins. Evidence for nonequivalent iron(III) sites. Proc Natl Acad Sci U S A 71:125-127

Rögner, M, Nixon, PJ, Diner, BA (1990) Purification and characterization of photosystem I and photosystem II core complexes from wild-type and phycocyanin-deficient strains of the cyanobacterium *Synechocystis* PCC 6803. J Biol Chem 265:6189-6196

Schreiber, U and Klughammer, C (2016) Analysis of photosystem I donor and acceptor sides with a new type of online-deconvoluting kinetic LED-array spectrophotometer. Plant Cell Physiol 57:1454-1467

Schreiber, U, Schliwa, U, Bilger, W (1986) Continuous Recording of Photochemical and Nonphotochemical Chlorophyll Fluorescence Quenching with A New Type of Modulation Fluorometer. Photosynth Res 10:51-62

Schreiber, U (2017) Redox changes of ferredoxin, P700, and plastocyanin measured simultaneously in intact leaves. Photosynth Res 134:343-360

Schreiber, U, Klughammer, C, Neubauer, C (1988) Measuring P700 absorbance changes around 830 nm with a new type of pulse modulation system. Z Naturforsch 43c:686-698

Sétif, P (2001) Ferredoxin and flavodoxin reduction by photosystem I. Biochim Biophys Acta 1507:161-179

Sétif, P (2015) Electron-transfer kinetics in cyanobacterial cells: Methyl viologen is a poor inhibitor of linear electron flow. Biochim Biophys Acta 1847:212-222

Sétif, P, Mutoh, R, Kurisu, G (2017) Dynamics and energetics of cyanobacterial photosystem I:ferredoxin complexes in different redox states. Biochimica et biophysica acta 1858:483-496

Srinivasan, N and Golbeck, JH (2009) Protein-cofactor interactions in bioenergetic complexes: The role of the A_{1A} and A_{1B} phylloquinones in Photosystem I. Biochim Biophys Acta 1787:1057-1088

Stephens, PJ, Thomson, AJ, Keiderling, TA, Rawlings, J, Rao, KK, Hall, DO (1978) Cluster characterization in iron-sulfur proteins by magnetic circular dichroism. Proc Natl Acad Sci U S A 75:5273-5275

Tagawa, K and Arnon, DI (1968) Oxidation-reduction potentials and stoichiometry of electron transfer in ferredoxins. Biochim Biophys Acta 153:602-613

Vangelder, BF and Slater, EC (1962) Extinction Coefficient of Cytochrome C. Biochimica et biophysica acta 58:593-&

Witt, H, Bordignon, E, Carbonera, D, Dekker, JP, Karapetyan, N, Teutloff, C, Webber, A, Lubitz, W, Schlodder, E (2003) Species-specific differences of the spectroscopic properties of P700 - Analysis of the influence of non-conserved amino acid residues by site-directed mutagenesis of photosystem I from *Chlamydomonas reinhardtii*. J Biol Chem 278:46760-46771

Zhang, L, McSpadden, B, Pakrasi, HB, Whitmarsh, J (1992) Copper-mediated regulation of cytochrome c553 and plastocyanin in the cyanobacterium Synechocystis 6803. J Biol Chem 267:19054-19059

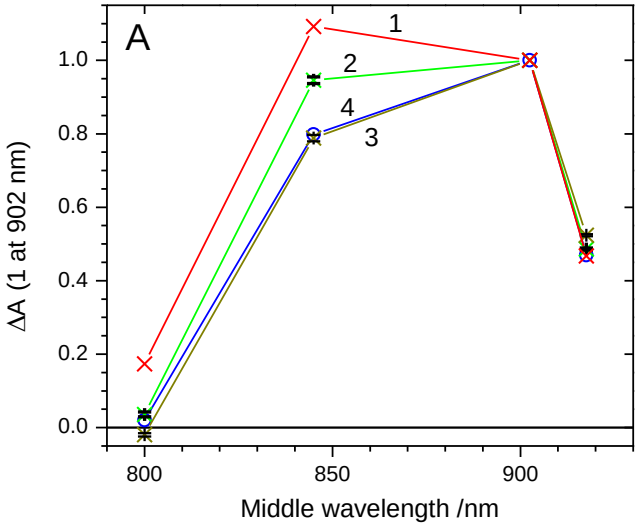
A
1
2
4
3
ΔA (1 at 902 nm)
1.0
0.8
0.6
0.4
0.2
0.0
800
850
900
Middle wavelength /nm

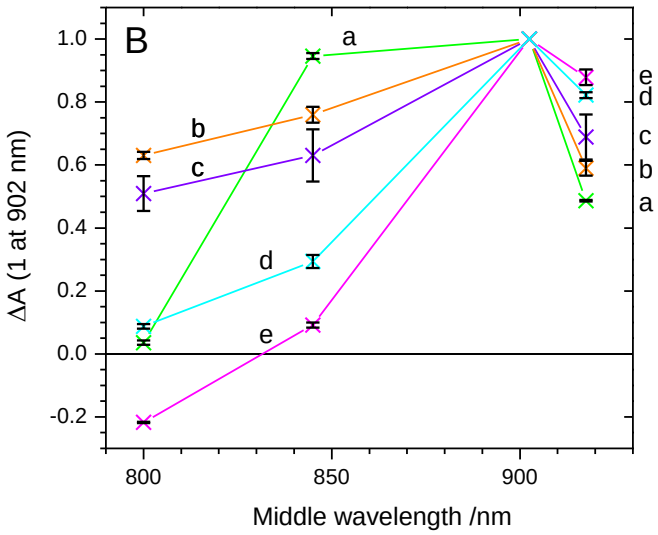
B
a
b
c
d
e
e
d
c
b
a
ΔA (1 at 902 nm)
1.0
0.8
0.6
0.4
0.2
0.0
-0.2
800
850
900
Middle wavelength /nm

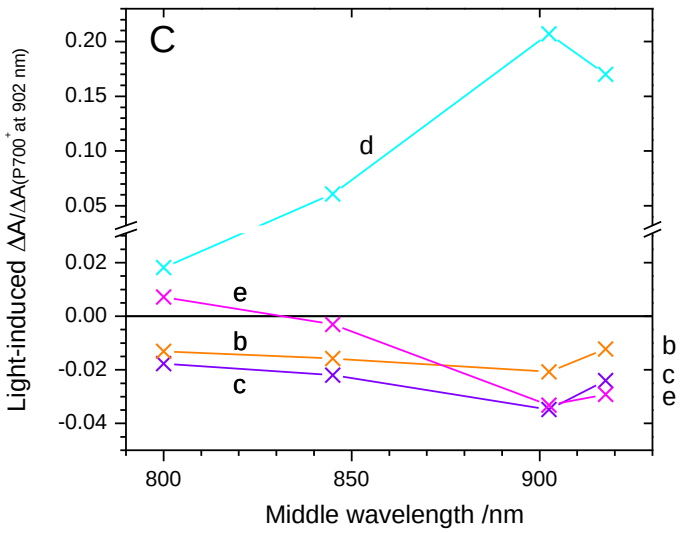
C
d
e
b
c
b
c
e
Light-induced ΔA/ΔA(P700+ at 902 nm)
0.20
0.15
0.10
0.05
0.02
0.00
-0.02
-0.04
800
850
900
Middle wavelength /nm

Fig. 1. Near-infrared pseudospectra measured *in vitro* with isolated proteins. The 4 middle wavelengths 800, 845, 902.5 and 917.5 nm correspond to the absorption change differences (780 nm – 800 nm), (820 nm – 870 nm), (840 nm – 965 nm) and (870 – 965 nm), respectively. **A**. $P700^+$ spectra (P does not contribute in the near-infrared region) normalized to 1 at 902.5 nm for PSI monomers from *Syn.* 6803 (1, red crosses), PSI trimers from *T. elong*. (2, green crosses, average of 5 spectra), tobacco (3, dark yellow crosses, average of 3 spectra) and *Helianthus annuus* (4, blue circles). **B**. Redox difference spectra normalized to 1 at 902.5 nm. The Pcy spectrum was measured with the spinach enzyme whereas all other spectra were obtained with *T. elong*. proteins. a, $P700^+$ (same as 2 in part A); b, orange, Fd, average of 3 spectra; c, violet, (F_A F_B), average of 5 spectra; d, cyan, Pcy, average of 2 spectra; e, magenta , cyt. c_6, average of 2 spectra. Standard deviations are indicated in A and B except for $P700^+$ of *Syn.* 6803 (1 measurement) and of *Helianthus annuus* (given with the KLAS-NIR software). **C**. Light-induced spectra (*i.e*. oxidized minus reduced for Pcy and cyt. c_6 and reduced minus oxidized for Fd and (F_A F_B)). Same spectra as in part B with identical colors and letters. The (F_A F_B) difference spectrum corresponds to single (F_A F_B) reduction. The spectra of cyt. c_6, (F_A F_B) and Fd were scaled to that of *T. elong.* $P700^+$ whereas the spectrum of Pcy was scaled to that of tobacco $P700^+$ (both $P700^+$ = 1 at 902.5 nm).

	Absorption pseudo-coefficients at 902.5 nm by reference to *T. elong*. $P700^+$	Absorption pseudo-coefficients at 902.5 nm by reference to tobacco $P700^+$
$P700^+$	1	1
Pcy_{ox} - Pcy_{red}	n.d.[(a)]	0.207 ± 0.004
cyt. c_{6ox} – cyt. c_{6red}	-0.033 ± 0.006	-0.034 ± 0.004
$(F_A\ F_B)_{1red}$ - $(F_A\ F_B)_{ox}$	-0.036 ± 0.008	-0.0335 ± 0.004
Fd_{red} - Fd_{ox}	-0.021 ± 0.005	-0.020[(b)]

Table 1. Relative differential absorption coefficients at 902.5 nm (840 nm – 965 nm).

(a): not determined. (b): single measurement. Standard deviations correspond to averages of 2 to 4 measurements.

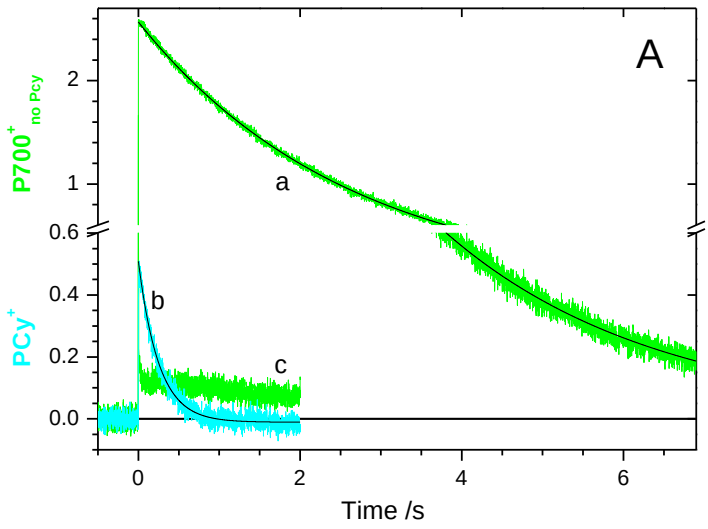
A
P700+ no Pcy
PCy+
a
b
c
Time /s

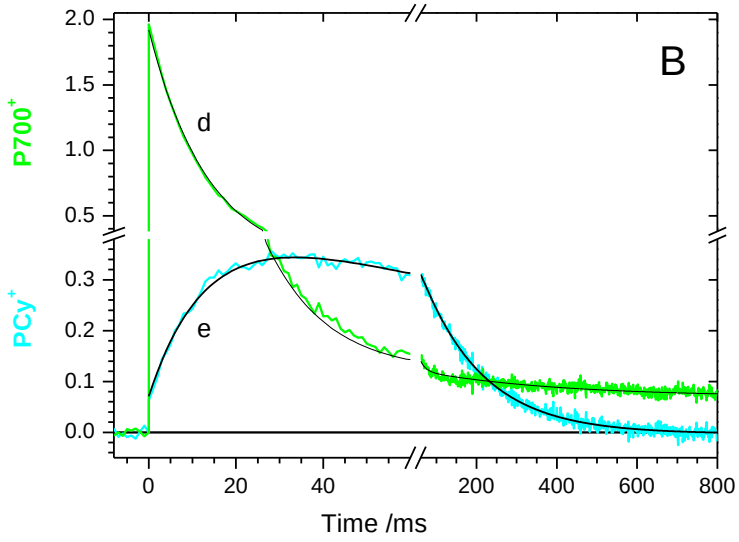
B
P700+
PCy+
d
e
Time /ms

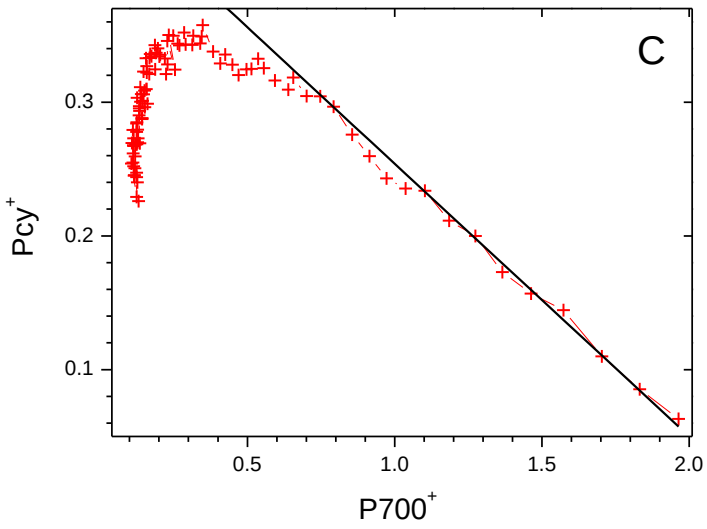
C
Pcy+
P700+

Fig. 2. Redox changes of P700 (green traces a, c and d) and Pcy (cyan traces b and e) (2-species deconvolution) measured with PSI and PCy isolated from tobacco and spinach, respectively. Measurements were made in the presence of 1 mM sodium ascorbate, 3 µM DCPIP and 1 mM MV. Excitation was provided by a single turnover laser flash. **A**. Trace a attributed to $P700^+$: 0.24 µM PSI (no Pcy). Trace b and c: 0.24 µM PSI, 8.2 µM Pcy. Trace b is attributed to PCy^+ whereas trace c is a minor $P700^+$ component not reducible by Pcy (see text). Signals decays a and b were fitted with monoexponential functions (black traces) giving amplitudes of 2.568 and 0.509, respectively (rates of 0.383 and 3.98 s^{-1}). Signals are averages of 10 measurements (Δt = 20 s). **B**: 0.21 µM PSI, 0.82 µM Pcy. Traces d and e are attributed to $P700^+$ and PCy^+, respectively. They were fitted together in a global fitting procedure with a common fast component (decay for $P700^+$ and rise for PCy^+: k= 73.5 s^{-1}) and one slow decay component, which is different for each species (k = 2.94 and 6.58 s^{-1} for $P700^+$ and PCy^+, respectively). Average of 50 measurements (Δt = 20 s). **C**. Pcy^+ was plotted as a function of $P700^+$ from part of the data in B (from 0 to 100 ms). The line corresponds to a ($Pcy^+/P700^+$) ratio of 0.204 that was calculated from the data fit of part B (see text).

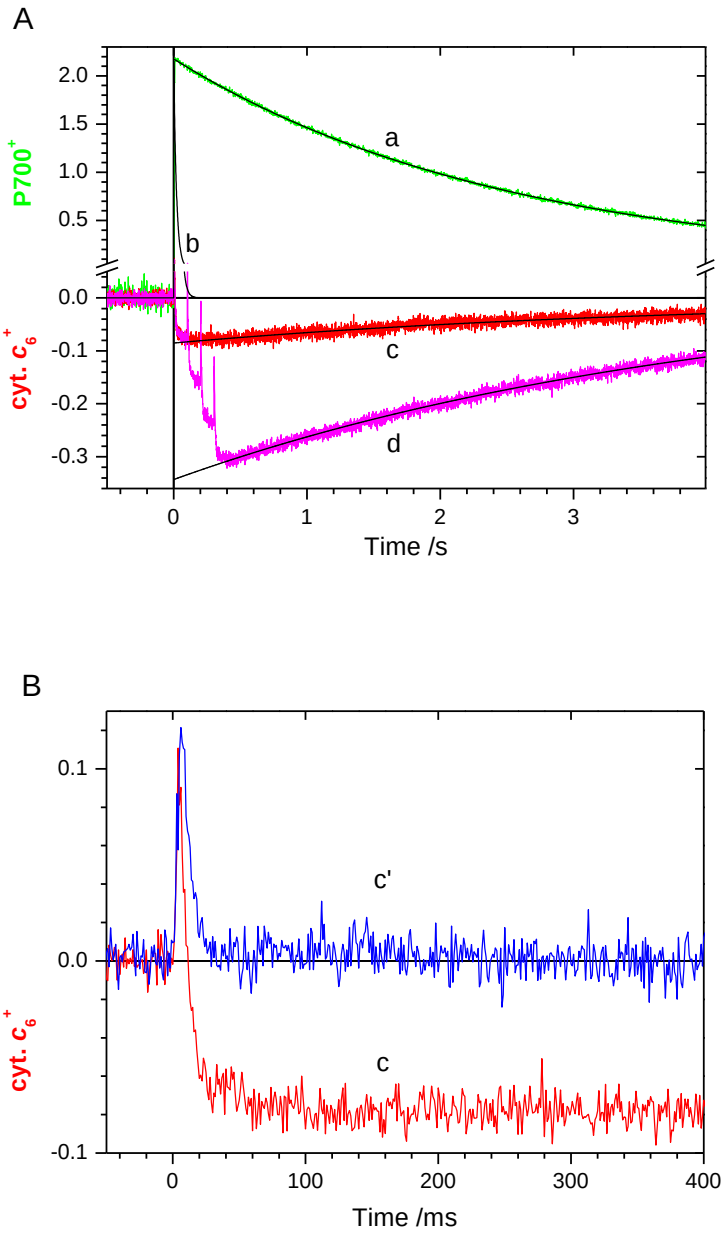

Fig. 3. Redox changes of P700 (traces a and b) and cyt. c_6 (traces c, c' and d) measured with isolated PSI and cyt. c_6 from *T. elong.* after 2-species deconvolution. All measurements were performed in the presence of 1.3 mM sodium ascorbate and 100 µM MV. **A**. Trace a: 0.21 µM PSI, 20 µM DCPIP (no cyt. c_6), 50 µs ST flash. Traces b to d: 0.21 µM PSI, 8.3 µM cyt. c_6, (no DCPIP). Single (traces a to c) or four (trace d) 100 ms-separated 50 µs ST flashes. Initial amplitudes from fits with monoexponential decays (black traces) : 2.176 ($P700^+$, trace a), 2.154 ($P700^+$, trace b), -0.085 (cyt. c_6, trace c) and -0.343 (cyt. c_6, trace d). The best fit of trace b gives a $t_{1/2}$ of 14.7 ms. **B**. Trace c is the same as in part A on a smaller time scale whereas trace c' was recorded after the addition of 10 µM DCPIP. Traces result from averages of 40 measurements (Δt = 15 s) except trace a (10 measurements, Δt = 30 s).

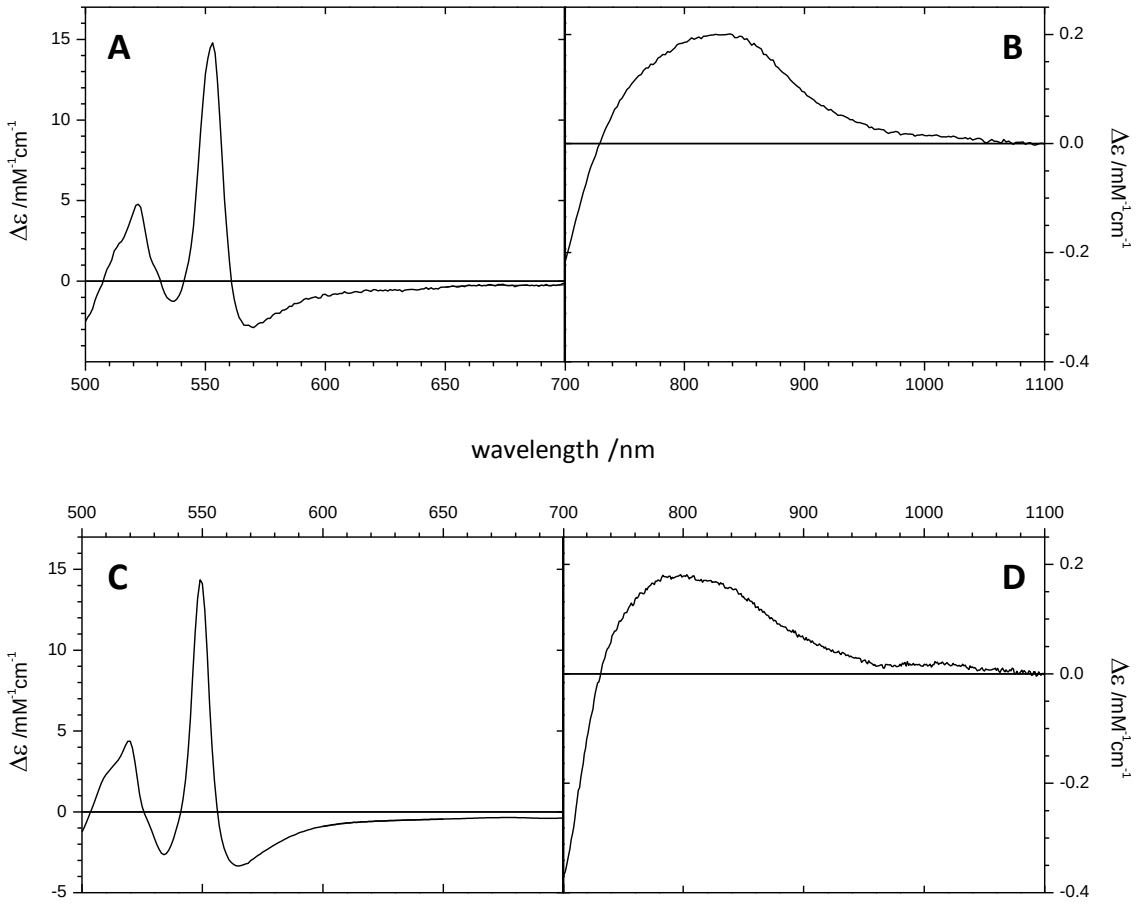

Fig. 4. Redox difference spectra (reduced minus oxidized) of cyt. c_6 (A and B) and horse heart cyt. *c* (C and D) between 500 and 1100 nm. Vertical scaling was made by assuming a coefficient of 100 $mM^{-1}cm^{-1}$ for reduced cytochromes at the Soret band maximum (415-416 nm, not shown). Cytochrome concentrations of 60 and 600 µM were used for measuring the spectra in the 500-650 and 600-1100 nm regions, respectively. As prepared cytochromes were oxidized with potassium ferricyanide and reduced with sodium ascorbate.

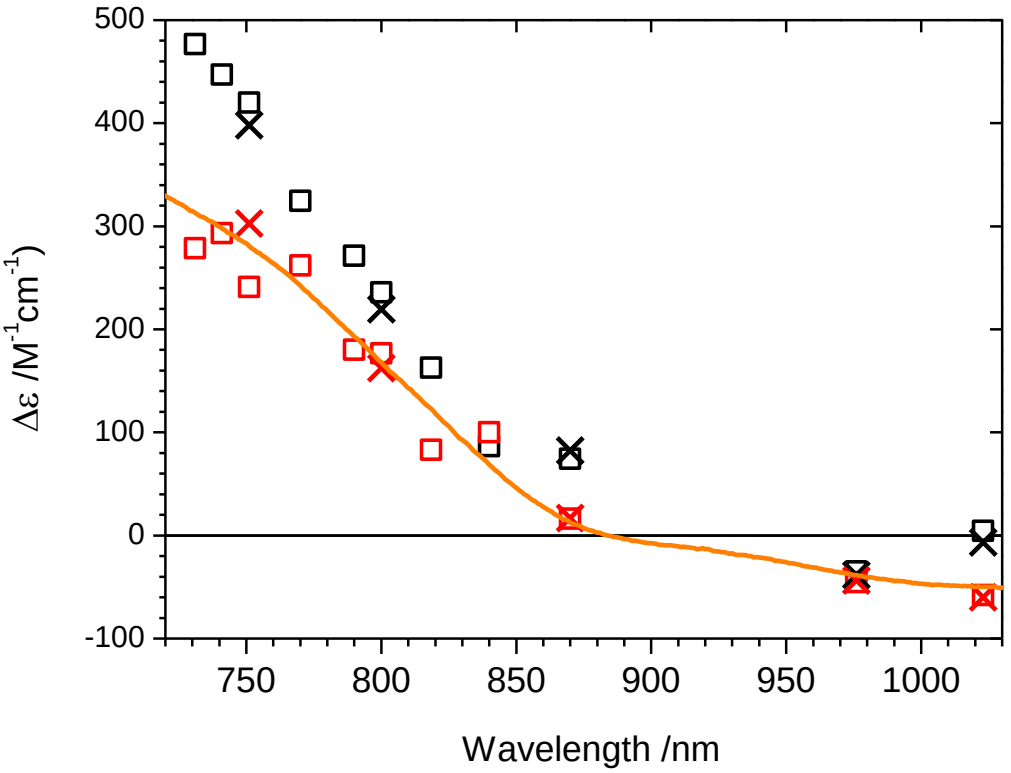

Fig. 5. Redox difference spectra (oxidized minus reduced) measured by flash-absorption spectroscopy. The spectra of (F_A F_B) (single reduction) and Fd were measured with PSI and Fd isolated from *T. elong.* from experiments similar to those described in Fig. SI3. Black and red symbols correspond to (F_A F_B) and Fd, respectively. Open squares, crosses and triangles were measured with three different samples. Vertical scaling was obtained using a coefficient of 7.7 $M^{-1}cm^{-1}$ for $P700^+$ at 800 nm. The orange spectrum is the Fd difference spectrum obtained by chemical reduction of Fd (3 mM sodium dithionite at pH 9.0) measured with a Fd concentration of 435 µM.

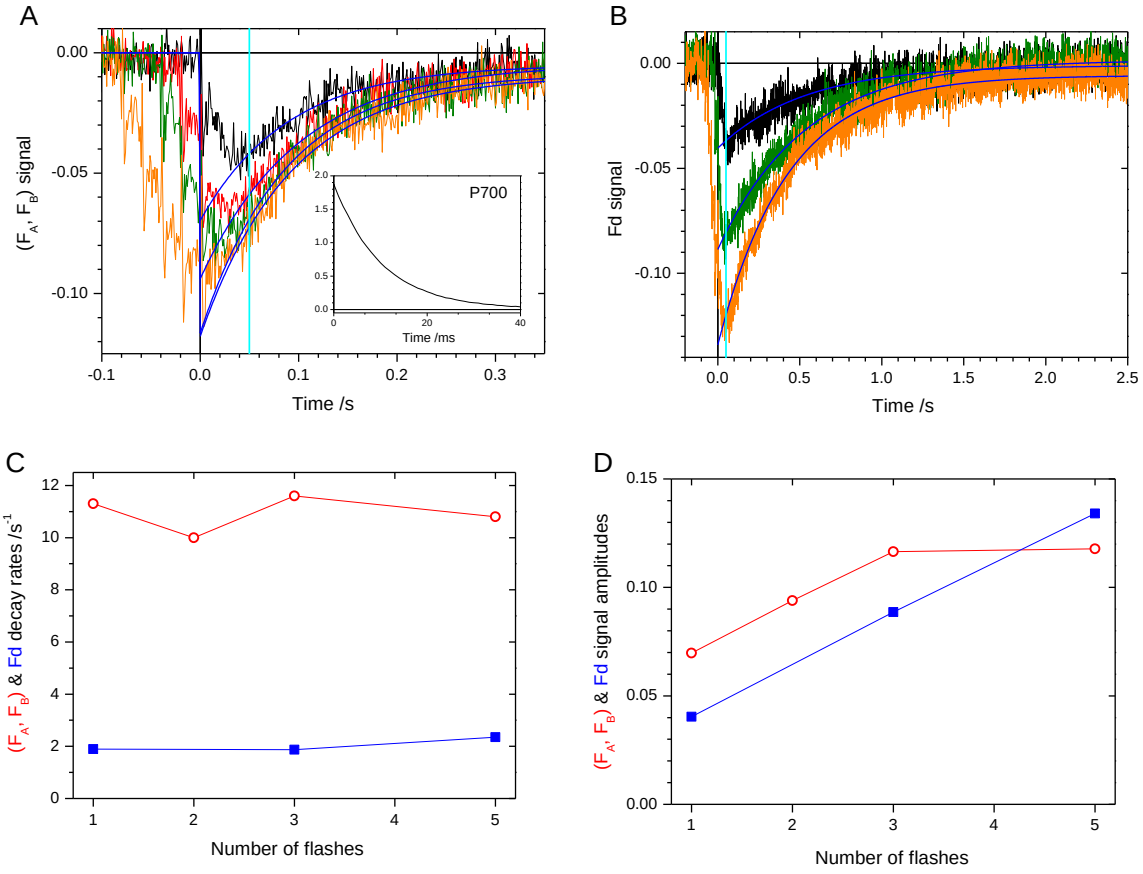

Fig. 6. Multiple flash (F_A F_B) and Fd reduction measured with isolated PSI, cyt. c_6 and Fd from *T. elong.* in the presence of DCPIP. All measurements were performed in the presence of 1.3 mM sodium ascorbate and 10 µM DCPIP with 0.175 µM PSI and 25 µM cyt. c_6, either in the presence of 10 µM Fd (part B) or in its absence (part A). Series of 50 µs ST flashes separated by 20 ms time intervals were used. Time 0 is defined as the time of the last flash of the series. **A**. (F_A F_B) kinetics were obtained after 3-species deconvolution (P700, cyt. c_6 and (F_A F_B)) (see text). Increasing signal amplitudes correspond to 1, 2, 3 and 5 ST flashes (black, red, green and orange, respectively). Monoexponential fits of the (F_A F_B) signal decays were performed (blue lines) using data only after 50 ms (cyan vertical line) due to signal distortions at shorter times (see text). The inset shows the $P700^+$ decay after a single ST flash. **B**. Fd kinetics were obtained after 3-species deconvolution (P700, cyt. c_6 and Fd). Increasing signal amplitudes correspond to 1, 3 and 5 ST flashes (black, green and orange, respectively). Monoexponential decay fits were performed as in part A using the Fd_{red} data after 50 ms. **C**. Decay rates of $(F_A\ F_B)_{red}$ and Fd_{red} obtained from the fits in parts A and B. **D**. Initial amplitudes (extrapolated to time 0) obtained from the fits in parts A and B. All kinetics traces result from averages of 80 experiments (Δt = 10 s).

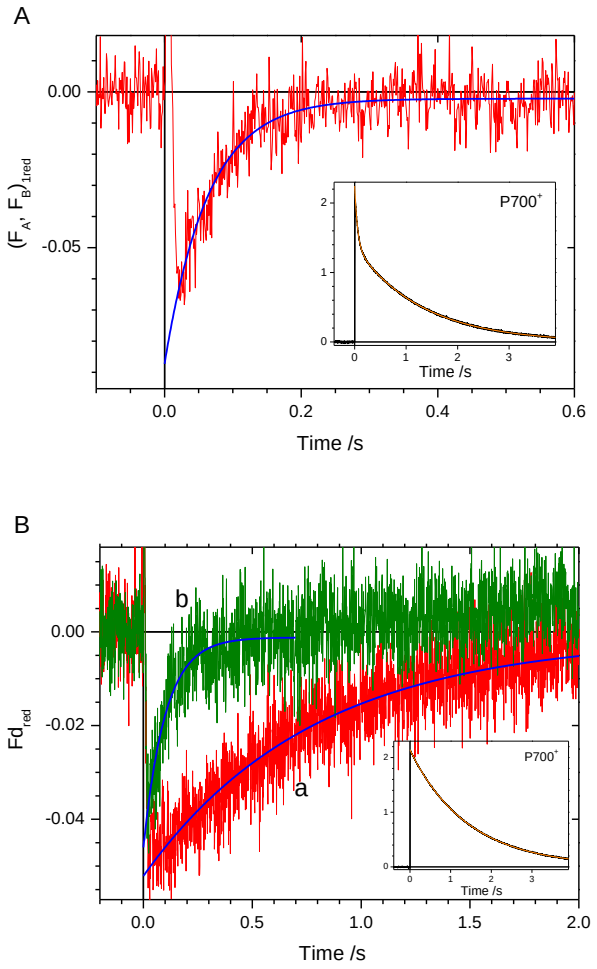

Fig. 7. (F_A F_B) and Fd reduction following a single 50 µs ST flash in the absence of cyt. c_6. Signals were measured with isolated PSI (0.206 µM) without Fd (part A) or with Fd (part B) (proteins from *T. elong.*) in the presence of 2 mM sodium ascorbate and 20 µM DCPIP. **A**. $(F_A\ F_B)_{1red}$ formation and decay was obtained from 2-species deconvolution (P700 and (F_A F_B)). The $P700^+$ signal is shown in the inset. Its biphasic decay was fitted with 2 exponential components. The fastest component (17.6 s^{-1}) corresponds to the sum of the rates of recombination and $(F_A\ F_B)_{1red}$ escape reactions (see text). $(F_A\ F_B)_{1red}$ was fitted with a single component of same rate (blue curve) using data only after 25 ms due to signal distortions at shorter times. Fit extrapolation at time 0 gives an amplitude of -0.087 (*vs* 2.244 for $P700^+$). **B**. 15 µM Fd was added to the cuvette studied in A (corresponding to PSI dilution by a factor of 1.05). Fd_{red} formation and decay (red trace a) was obtained from 2-species deconvolution (P700 and Fd). The $P700^+$ signal is shown in the inset. Its monophasic decay was fitted by a single exponential leading to an initial amplitude of 2.141. Fd_{red} decay was also fitted by a single exponential (blue curve: rate 1.28 s^{-1}, initial amplitude -0.052). Then 0.5 µM MV was added to the cuvette (negligible sample dilution), leading a faster Fd_{red} decay (green trace b) which was fitted by a single exponential (rate 9.9 s^{-1}, initial amplitude -0.046). All kinetic traces result from averages of 80 measurements (Δt = 10 s).

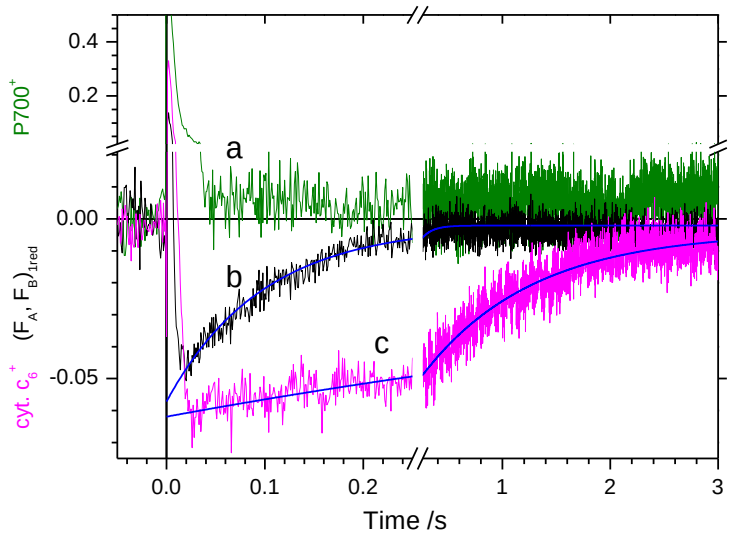

Fig. 8. (F_A F_B) reduction and cyt. c_6 oxidation following a single 50 µs ST flash in the absence of DCPIP. Signals were measured with isolated PSI and 48 µM cyt. c_6 in the presence of 2 mM sodium ascorbate. The PSI concentration (0.16 µM, signal size of 1.77) was calculated from the $P700^+$ signal which was measured with a sample of identical concentration containing DCPIP but no cyt. c_6. The P700, (F_A F_B) and cyt. c_6 signals (a/green, b/black and c/magenta, respectively) were obtained after 3-species deconvolution. $(F_A\ F_B)_{1red}$ and cyt. c_{6ox} decays were fitted with monoexponential functions using data after 25 ms. The decay rates and initial amplitudes given by the fits were the following: 10.3 s^{-1} and -0.057 for (F_A F_B), 0.98 s^{-1} and -0.062 for cyt. c_6. All traces result from an average of 80 measurements (Δt = 10 s).